


Jessica Köpplin*
Lena Bednarz
Thomas Hagemeyer*
Dominique Thévenin

Fluorescence Imaging Methodology for Oil-in-Water Concentration Measurements

A Pitot-tube jet pump for separating and transporting liquids of different densities is in use for processing oil-polluted water. The remaining oil-in-water (OiW) concentration is a main indicator for the process efficiency and requires a precise measuring method. Hence, a simple approach delivering reliable oil concentrations has been developed in this project. The measurement principle relies on the image acquisition of an OiW emulsion, where the oil phase is seeded with a selective dye tracer. In this concept study, a detailed description of the preparation procedure is provided. Suitable operation parameters leading to sufficiently stable emulsions have been obtained. Finally, a calibration function was determined. It can be used to correlate uniquely the image intensity to the oil concentration.

 This is an open access article under the terms of the Creative Commons Attribution-NonCommercial License, which permits use, distribution and reproduction in any medium, provided the original work is properly cited and is not used for commercial purposes.

Keywords: Emulsion stability, Homogenization, Fluorescence image analysis, Oil-in-water emulsion

Received: January 19, 2021; *revised:* March 26, 2021; *accepted:* May 05, 2021

DOI: 10.1002/ceat.202100023

1 Motivation and Background

Oil-in-water (OiW) emulsions are a kind of multiphase flows, which can be found with different morphologies in uncountable applications, mainly for process, chemical, and environmental engineering; see, e.g., [1, 2]. The desired states for OiW emulsions differ widely. In many industrial applications, a homogeneous mixture of different oils and water is desired. Hence, the system requires intense shearing and dispersion to produce a stable emulsion for a long time. On the other hand, the presence of mineral oils – even at very low concentrations – is a major threat for drinking water as well as for natural systems (lakes, rivers, seawater, etc.) [3]. Consequently, the separation of the oil phase from the water phase is one central objective of water treatment. For instance, bilge water treatment is found in every ship.

Improving the efficiency of separation devices, like the modified Pitot-tube jet pump (PTJ pump) considered in this study, is therefore very important and still an ongoing process. The modified Pitot-tube jet pump is an innovative solution for integrating oil-water separation and transport of the two separated phases. It has been developed in our group within the last years, in cooperation with an industrial partner [4–6].

It is possible to achieve a high separation efficiency of the pumped water using the PTJ pump, as demonstrated by preliminary experiments [5]. In order to check the impact of process and device modifications, highly accurate measurement results of the OiW concentrations are required. In particular, a reliable estimation at very low concentrations is necessary. For instance, the upper threshold for bilge water release in the environment according to the MARPOL regulation is only 15 ppm oil in water [7].

The liquid-liquid separation, e.g., oil-water separation, can be achieved in different ways. Centrifuges are common for solid-liquid separation but can be also used for liquid-liquid separation [8, 9]. The attention of recent research is mostly set on hydrocyclone separation, as reviewed, e.g., by Kharoua et al. [10–12]. In this work, the authors investigate important operation parameters for hydrocyclone separation and provide information regarding the obtained performance. Most commonly, the hydrocyclone separation process is controlled using the pressure drop ratio [13], which is an indirect measure of separation efficiency.

But there are other techniques, like impedance tomography [14] or direct droplet size characterization and counting methods [15], to monitor the resulting OiW concentration. The patent description of Perfect et al. [16] contains a general overview of existing methods to characterize the composition of liquid-liquid multiphase flows. A survey on fluorescence-based OiW monitors, in particular on the calibration procedure, concentration ranges, and real-time applicability is provided by Lambert [17]. The author elaborates in particular on various portable devices, which are commercially available and usually applied for monitoring the natural fluorescence of hydrocarbons. Moreover, this review paper clearly states the difficulties associated to the calibration procedure for fluorescence measurements and the lack of a detailed documentation.

Jessica Köpplin, Lena Bednarz, Dr.-Ing. Thomas Hagemeyer, Prof. Dr.-Ing. Dominique Thévenin,
jessica.koepplin@ovgu.de, Thomas.Hagemeyer@ovgu.de
Lab. of Fluid Dynamics & Technical Flow, Otto von Guericke University Magdeburg, Universitaetsplatz 2, 39106 Magdeburg, Germany.

More recently, Durdevic et al. [18] published a study on a dynamic measurement technique for low OiW concentrations (below 1%). This feasibility study describes the successful application of a fluorescence-based oil concentration monitoring device for feedback control of a hydrocyclone oil-water separation plant. The authors report a quick response (3 s) for the commercial device they employ. However, they also underline the importance of validating the results with a different measurement principle.

The central objective of the work described in this paper is to establish a simple but reliable procedure for measuring the OiW concentration using an imaging technique.

2 Experimental Setup and Methodology

2.1 Experimental Setup

The generation of an oil-water mixture, which is stable for a sufficient time without the application of an emulsifier, requires a high-energy mixing device. In this project, a Polytron PT3100 was applied for homogenization of the oil-water mixture.

The preparation process was identical for all tests carried out during this study. A volume of 200 mL deionized water was mixed with a known amount of commercial sunflower oil to create a desired OiW concentration sample (see Tab. 1 for exact quantities). The sunflower oil is seeded with a selective fluorescent dye tracer “Nile Red” (CAS No. 7385-67-3), at a dye concentration in oil of 10 mg L^{-1} . This tracer dye is insoluble in water [19]. The sunflower oil containing the fluorescent dye tracer is filtered before mixing with water to remove any remaining solids, which may otherwise disturb the fluorescence signal. Due to its selective solubility, the dye tracer is a marker for the oil phase within the oil-water mixture.

Fluorescence imaging requires the knowledge of a transfer or calibration function that correlates the fluorescence intensity to the quantity of interest. Generally, fluorescence imaging relies on a constant illumination of homogeneously distributed particles, which emit light in the corresponding fluorescence bandwidth. For further details on the fundamentals of fluorescence imaging, the interested reader is referred to the work of Hagemeyer et al. [20, 21].

In contrast to conventional applications, where an isotropic distribution of the fluorescent dye tracer in the continuous

fluid is used, the procedure in this study uses a fluorescence marker in the dispersed phase within an emulsion.

Therefore, the application of fluorescence imaging requires monodispersed oil droplets homogeneously distributed in the emulsion sample. This ensures constant optical properties of the fluorescence light emitted by the emulsion droplets. Preliminary studies revealed conditions and parameters for the preparation of a homogeneous emulsion with temporally limited stability. The employed preparation process ensured a homogeneous and temporally stable emulsion for a suitably long time to carry out further optical investigations.

During these preliminary experiments, the mixture was prepared freshly for every new test with different conditions, using always new components to avoid any possible contamination. The oil-water mixture was stirred at a mixing speed between 6000 and 12 000 rpm for durations in the range of 15–180 s to evaluate the required mixing energy and time. The energy transferred from the stirrer to the mixture leads to a dispersion of the oil phase within the water phase. The oil droplet size becomes smaller with higher mixing intensity, i.e., increased momentum transferred from the stirrer. Smaller oil droplets correspond to a much slower rising velocity due to buoyancy within the continuous water phase, so that the stability of the resulting emulsion is ensured for a longer time.

The main objective of these preliminary tests was to identify the time scale on which the assumption of a homogeneous oil distribution in the sample is justified. Based on the obtained results, the samples used for the fluorescence imaging experiments have been always prepared with a mixing speed of 12 000 rpm and a mixing duration of 30 s. These parameters provide homogeneous emulsions and stable conditions for the whole duration of one experiment, including filling the cuvette, arranging it within the setup, and acquiring images.

Fig. 1 shows the setup of the imaging system. Samples produced in the aforementioned way were placed in front of a CMOS camera (FLIR Blackfly S, mono, 5 MP). The CMOS camera acquires grayscale images in a 16-bit range. Accordingly, the brightness of an individual pixel takes a value between 0 and 65 535 of the grayscale range.

The camera is equipped with Nikon F60 objective lens operating with an f number of 2.8 and at a scale factor of $59.7 \text{ pixel mm}^{-1}$. Additionally, a 580-nm high-pass filter is installed onto the objective lens. The filter has been selected in compliance with the fluorescence spectrum of Nile red in sunflower oil and the illumination source. For fluorescence excita-

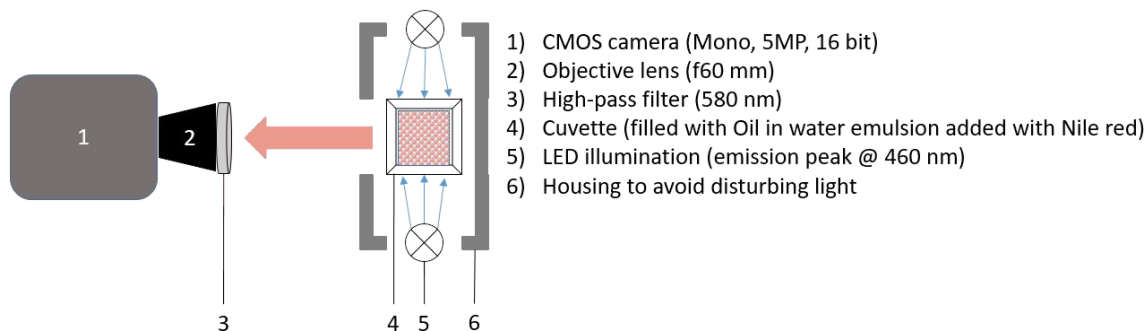


Figure 1. Schematic setup of the fluorescence imaging methodology for OiW concentration measurements.

tion, two vertically aligned bands of blue light-emission diodes (LEDs; emission peak at 460 nm) have been installed to the left and right of the cuvette. They ensure an intense and continuous illumination of the cuvette from both sides, which is mandatory to achieve homogeneous fluorescence excitation. A black cardboard frame is arranged around the cuvette to reduce disturbance from ambient light.

2.2 Experimental Procedure for Oil Concentration Measurements

Finally, a test series investigated the influence of the oil concentration on the fluorescence intensity and distribution for suitable constant rotation speed and mixing time, as determined by the preliminary investigations, i.e., all mixtures have been homogenized during 30 s at 12 000 rpm to achieve a stable emulsion during a time sufficient for further optical investigation. These final tests used the same pure sunflower oil seeded with a constant fluorescent dye tracer of 10 mg of Nile-Red for 1 L of sunflower oil. Then, seven samples of oil-water mixtures with different OiW concentrations were prepared.

The oil concentration was controlled using a high-accuracy balance (RADWAG; measurement precision of 0.1 mg). In this way, it was possible to prepare oil-water mixtures containing 200 mL of water and a corresponding amount of sunflower oil. The sunflower oil density was measured as 865 kg m^{-3} , which leads to a volumetric concentration of $1.15 \times 10^{-4} \text{ L}$ of oil per liter of water for the absolute oil content of 0.02 g. This concentration can be also expressed in ppm, which yields a value of 100 ppm for the absolute oil content of 0.02 g. Tab. 1 summarizes the corresponding values for all cases.

2.3 Image Processing Algorithm

For image processing, an image analysis algorithm has been coded using Matlab environment (Version R2019, from The MathWorks Inc.). The algorithm sequence is displayed in Fig. 2. The image processing sequence starts by reading the raw

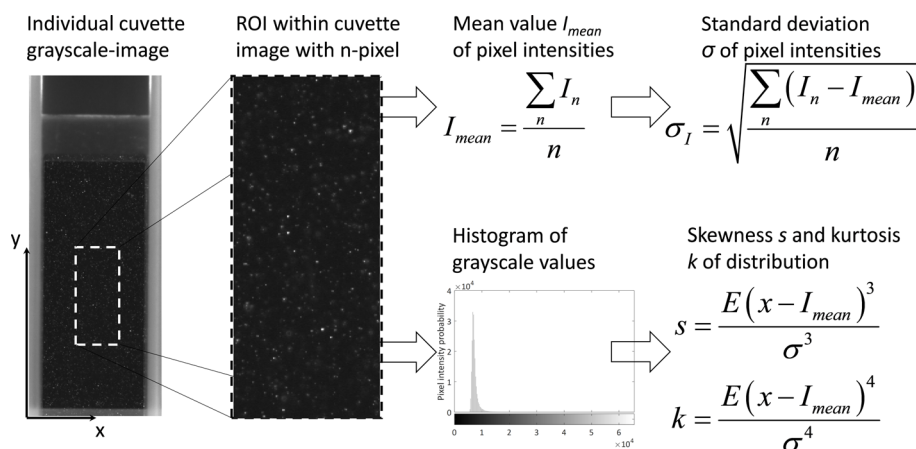


Figure 2. Schematic drawing of the image processing algorithm including all individual steps ordered from left to right. It starts with a grayscale image, where an ROI has to be defined (white rectangle). For this area, the calculation of mean value and standard deviation is carried out. Additionally, the histogram of the grayscale values is analyzed for its skewness and kurtosis.

images, which come as grayscale images. The grayscale is directly proportional to the fluorescence signal produced by the sample illuminated in the cuvette. Subsequently, a region of interest (ROI) is automatically set. This is necessary to avoid regions with strong optical distortion near the edges of the cuvettes. Since all cuvettes were located exactly at the same place, the ROI always corresponds to identical pixel regions within the image, i.e., 400 pixels in x -direction (horizontal) and 500 pixels in y -direction (vertical), leading to 200 000 pixels in total. Grayscale intensities (average value of pixel intensity) and distribution (standard deviation of pixel intensity) have been evaluated for this area. Finally, the resulting intensity value is correlated with the known OiW concentration.

Later on in a detailed analysis, the histogram of the grayscale values within the ROI is calculated. The structure of this histogram was found to correlate with the oil concentration and may be used for further clarification of the exact oil concentration.

3 Experimental Results and Discussion

First experiments with constant OiW concentrations (1 mL oil per 200 mL water) have been used to assess the temporal stability. Different mixing intensities lead to emulsions with varying oil distribution and temporal stability. A global characterization of the mixing efficiency can be obtained from images that have

Table 1. Conversion table for different oil concentrations.

Sample	Sample 1	Sample 2	Sample 3	Sample 4	Sample 5	Sample 6	Sample 7
Absolute oil content [g]	0.002	0.01	0.02	0.05	0.1	0.15	0.2
Exact mass concentration [g L^{-1}]	0.01	0.05	0.1	0.25	0.5	0.75	1
Exact volume concentration [L L^{-1}]	1.15×10^{-5}	5.78×10^{-5}	1.15×10^{-4}	2.89×10^{-4}	5.78×10^{-4}	8.67×10^{-4}	1.15×10^{-3}
Exact mass concentration [ppm]	10	50	100	250	500	750	1000

been acquired directly after the mixing ended (corresponding to time t_0).

Fig. 3 indicates the initial state of the emulsion for mixing speeds between 6000 and 12 000 rpm. Obviously, mixing below 10 000 rpm is not sufficient for homogenization of the oil-phase within the water. A significant oil layer exists at the surface of the liquid mixture. In contrast, an apparently homogeneous emulsion with sufficient temporal stability is achieved when mixing at 10 000 and 12 000 rpm, justifying again why the latter value has been retained for all final experiments.



Figure 3. Initial state of the emulsion as obtained immediately after homogenization at 6000, 8000, 10 000, and 12 000 rpm (from left to right) during 30 s.

The colored images in Fig. 3 have been captured in addition to the fluorescence images in order to visualize the very fast oil-water separation found at lower homogenization intensity (rotation speed lower than 10 000 rpm). Repeating several times these experiments it was possible to exclude any influence of preparation and handling of the samples on the final results. Using single-use pipettes avoids any kind of pollution during the filling procedure, but may lead to slightly different filling levels as seen in Fig. 3. However, the total volume or filling level in one cuvette does not affect the emulsion stability and the analysis since it is carried out for a representative area (ROI, white rectangle in Fig. 2), selected at a sufficient distance from all boundaries (liquid surface or walls).

3.1 Fluorescence Intensity Calibration

The homogenization process described up to now ensures a stable emulsion for a duration allowing suitable optical measurements. For the success of the project, the optical properties and in particular the fluorescence intensity should vary uniquely with the OiW concentration. A higher fluorescence intensity leads to a larger pixel intensity in the grayscale image when the oil concentration is higher, and vice versa. Accordingly, the fluorescence intensity is a measure for the OiW concentration, provided the corresponding calibration function is known. This conversion or calibration function uniquely relates the grayscale intensity of the image to the OiW concentration and is the central objective of this study, together with the corresponding procedure.

Fig. 4 presents the spatially averaged grayscale or fluorescence intensity I_{mean} as function of different oil concentrations directly after homogenization. From this figure it is clear that the intensity value correlates uniquely with the oil concentration; an increment in oil concentration leads to a clear increase

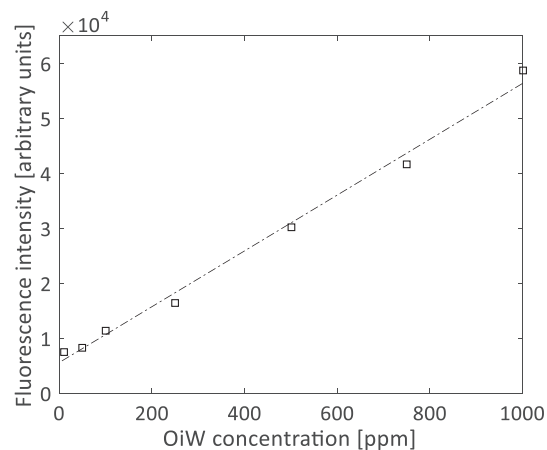


Figure 4. Fluorescence intensity (average grayscale value for the ROI given in grayscale unit between 0 and 65 535) as function of OiW concentration. For the horizontal axis, the OiW concentrations listed in Tab. 1 have been used.

of the intensity value. Hence, the image intensity can be safely used to measure the oil concentration.

Assuming a linear correlation between fluorescence signal and OiW concentration, a first-order polynomial function can be fitted to the measurements:

$$I_{\text{mean}} = a \cdot c + b \quad (1)$$

with the coefficients $a^{(1)} = 50.8$ in grayscale unit per ppm and $b = 5570$ in grayscale unit. The high quality of this fit can be quantified with $r^2 = 0.991$. The calibration function is plotted as dash-dotted line in Fig. 4. As the coefficients indicate, there is a background offset in the fluorescence intensity of 5570 grayscale unit. Moreover, the resolution is at 50.8 grayscale unit per ppm.

However, the optical method developed in this project is not capable to clearly distinguish OiW concentrations in the lowest concentration range (below 100 ppm) based only on the mean intensity. This is clearly visible in Fig. 4, in which the two symbols corresponding to the lowest oil concentrations show only minor difference regarding the measured intensity values. There are at least two solutions to overcome this issue. One solution would be to increase the dye concentration within the oil phase. This would result in an overall higher fluorescence intensity for all oil concentrations; however, one would lose information on the other end, due to saturation of the fluorescence signal for high oil concentrations.

Another way to overcome this issue is to take a closer look at the fluorescence or gray level intensity distribution. A lower oil concentration means less fluorescence light emitted by oil droplets within the emulsion. The intensity distribution of the images changes accordingly, such that there is a low number of bright pixels produced by single oil droplets aside of a large number of dark pixels, coming from the non-fluorescent water

1) List of symbols at the end of the paper.

content of the emulsion. This results in a highly skewed intensity histogram and is quantified by the corresponding higher-order moments of this distribution.

Exemplarily, the gray level distribution is depicted in Fig. 5 for the three lowest OiW concentrations. Obviously, the distribution functions differ significantly, even if the mean value shows only a difference of around 3000 (in grayscale unit of a 16-bit range). The structural difference in the intensity distribution functions can be better quantified using the higher-order moments, here the third- and fourth-order moments known as skewness and kurtosis.

The skewness and kurtosis of the intensity distribution functions can be correlated with the OiW concentration as well. They yield a much better insight for the lower concentration range and allow a detailed analysis for the OiW concentration over three decades (10 to 1000 ppm), with a constant dye concentration. The resulting correlation curves are illustrated below in Fig. 6. It can be seen that this procedure improves the information exactly where it is needed. Both, skewness and kurtosis values strongly increase with decreasing OiW concentration and can be fitted using a power law function with negative exponent.

The power law function used to fit the skewness of the fluorescence intensity PDF follows the form of:

$$\mu_{3,4} = a\alpha^b + c \quad (2)$$

with the coefficients $a = 24.49$, $b = -0.22$, and $c = -5.19$. The quality of the fit, $r^2 = 0.999$, is even better than for the mean intensity value. In a similar way, the results for the kurtosis of the fluorescence intensity PDF are fitted to the OiW concentration. The corresponding power law fit has the coefficients $a = 814.7$, $b = -0.68$, and $c = -6.82$ and a goodness of $r^2 = 0.999$.

In conclusion, the detailed description of the fluorescence intensity distribution as function of the OiW concentration permits oil concentration measurements in a wide concentration range, from 10 to 1000 ppm. An extrapolation or assignment even below 10 ppm seems possible. However, this concentration range was not investigated in this study. Further investigations will check the applicability as a function of camera settings and sensitivity.

For practical use, a first estimate of the oil concentration is possible based on the mean intensity. If this estimate turns out to be as low as 100 ppm or less, a second estimate based on the skewness or kurtosis of the fluorescence intensity PDF for clarification is suggested.

Tab. 2 provides a summary of the correlation values obtained for the individual OiW concentrations. The method to improve the discrimination of lower OiW concentrations revealed that there is a certain amount of fluorescence intensity saturation at the highest OiW concentration of 1000 ppm. Even if the average grayscale intensity and peak of the distribution function is well below the maximum value of the resolved intensity range ($\sim 65\,000$ in grayscale unit), a significant part of the PDF is cut off with the current setup. Accordingly, no values for skewness and kurtosis have been calculated for this case.

For a better understanding of how accurately fluorescence imaging works in this type of emulsions, even more detailed experiments are required. Generally, it is challenging to apply

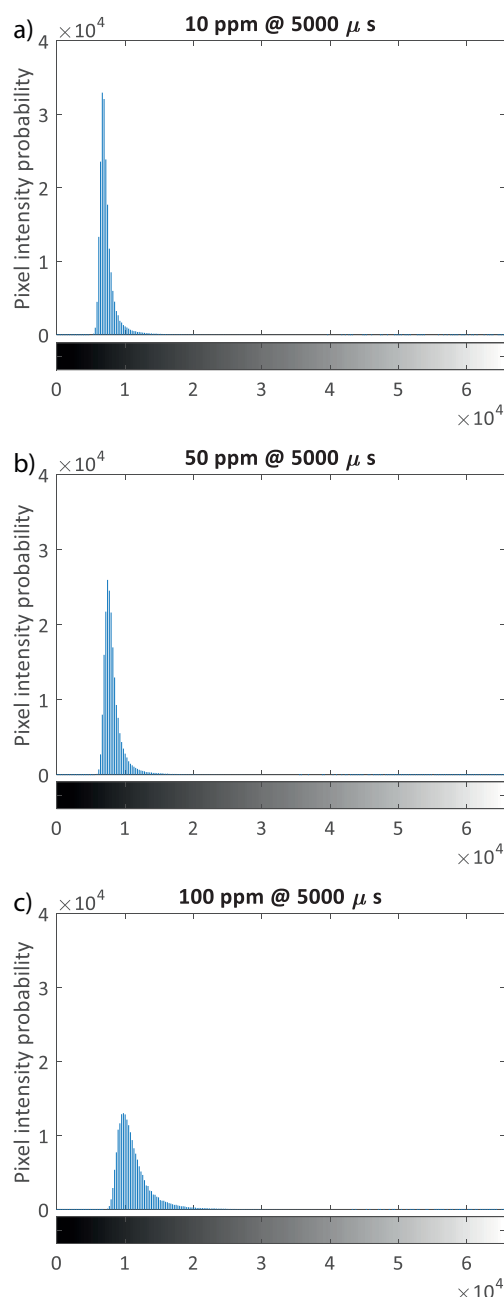


Figure 5. Probability density function (PDF) for the grayscale of the ROI pixels, exemplarily shown for OiW concentrations of 10, 50, and 100 ppm (ordered from top to bottom). The x-axis represents the grayscale level, which is provided in addition as legend below the x-axis.

optical measurement concepts in emulsions [22,23]. Accordingly, our future work will focus on coupling the fluorescence imaging with a microscopic analysis. Simultaneously acquired results can reveal the influence of the emulsion structure on the fluorescence signal.

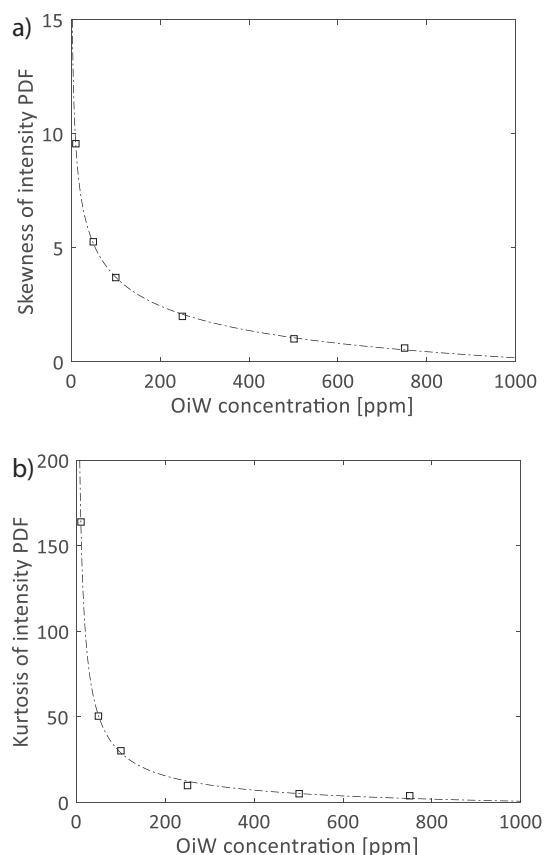


Figure 6. Correlation curves of skewness (top) and kurtosis (bottom) as function of the OiW concentration.

4 Conclusions

The procedure presented in this paper describes all steps required for accurate, image-based OiW concentration measurements. It is first essential to prepare homogeneous and sufficiently stable OiW emulsion samples, in order to enable reliable and accurate optical analysis. It has been shown that the homogenization process of sunflower oil and water is satis-

factory when stirring with at least 10 000 rpm for 30 s. The stability reached after homogenization at 12 000 rpm was sufficient for all optical measurements in this study. An even higher mixing intensity might lead to slightly increased stability of the emulsions and will be considered in future tests.

A longer mixing duration, i.e., more than 30 s, showed no benefits for the stability. It might ultimately lead to issues due to increased heat transfer and corresponding changes in the emulsion structure.

A detailed description of the emulsion sample preparation, stability, and calibration process was, to the best of our knowledge, not available in the literature yet. Moreover, this type of information is omitted usually in the technical description of commercial OiW concentration measurement and monitoring devices. Therefore, the findings of this study are valuable for an accurate quantification of low OiW concentrations down to 10 ppm as found, e.g., during the separation process using the modified Pitot-tube jet pump.

Transferring the findings of this study to an in-line concentration measurement concept relies on strictly conserving the setup and operating parameters of the offline methodology. However, the measurements become more complex. In particular, obtaining a thorough homogenization in an in-line arrangement will require additional investigations. Moreover, it is desirable to validate the concentration measurement results with other measurement principles, like oil droplet sizing and counting approaches.

Eventually, the fluorescence setup will be ready to perform in-line OiW concentration measurements in the pilot plant and allow for further optimization of the Pitot-tube jet pump separation technique.

Acknowledgment

This project is funded by the German Federal Ministry for Research (BMBF) as ZIM project (ZF4063102KO8). The authors gratefully acknowledge the technical support of Mrs. Schlüsselburg (TVT group) at the University of Magdeburg. Open access funding enabled and organized by Projekt DEAL.

The authors have declared no conflict of interest.

Table 2. Summary of OiW concentration and corresponding representation as mean grayscale intensity and higher-order moments of the intensity distribution.

Rounded OiW concentration [ppm]	I_{mean} [grayscale unit]	Third-order moment of PDF – skewness	Fourth-order moment of PDF – kurtosis
10	6682	9.556	163.875
50	7453	5.241	50.433
100	9766	3.712	30.234
250	14 649	2.001	9.981
500	28 784	1.0043	5.061
750	41 120	0.6121	3.641
1000	58 082	–	–

Symbols used

a	[grayscale unit; ppm]	coefficient in linear and power law fit (unit given for linear fit)
b	[grayscale unit]	coefficient in linear and power law fit (unit given for linear fit)
c	[-]	coefficient of power law fit
g	[m s ⁻²]	gravitational acceleration
I_{mean}	[grayscale unit]	grayscale intensity value
r^2	[-]	correlation coefficient of fit

Greek letters

α	[%]	oil concentration
μ	[-]	fit of skewness or kurtosis to OiW concentration
ρ	[kg m ⁻³]	mixture density

Abbreviations

OiW	oil in water
PDF	probability density function
PTJ	Pitot-tube jet (pump)
ROI	region of interest

References

- [1] G. Chen, D. Tao, *Fuel Process. Technol.* **2005**, *86* (5), 499–508. DOI: <https://doi.org/10.1016/j.fuproc.2004.03.010>
- [2] U. El-Jaky, M. F. Cunningham, T. F. L. McKenna, *Ind. Eng. Chem. Res.* **2009**, *48* (22), 10147–10151. DOI: <https://doi.org/10.1021/ie901005a>
- [3] C. Hu, C. Herz, R. L. Hartman, *Green Process. Synth.* **2013**, *2* (6), 611–623. DOI: <https://doi.org/10.1515/gps-2013-0085>
- [4] J. Meyer, L. Daróczy, D. Thévenin, *J. Fluids Eng.* **2017**, *139* (2), 021103/1–11. DOI: <https://doi.org/10.1115/1.4034455>
- [5] J. Meyer, Optimierung einer Pitot-Pumpe und deren Adaption zur Öl-Wasser-Trennung, *Ph. D. Thesis*, Otto-von-Guericke-Universität Magdeburg **2019**.
- [6] J. Meyer, D. Thévenin, in *Proc. of the 9th Int. Conf. on Multi-phase Flow* (Ed: A. Soldati), Firenze **2016**.
- [7] MARPOL 73/78, *International Convention for the Prevention of Pollution from Ships*, **1973**.
- [8] J. Lindner, H. Nirschl, *Sep. Purif. Technol.* **2014**, *131*, 27–34. DOI: <https://doi.org/10.1016/j.seppur.2014.04.019>
- [9] K. Menzel, J. Lindner, H. Nirschl, *Sep. Purif. Technol.* **2012**, *92*, 122–128. DOI: <https://doi.org/10.1016/j.seppur.2011.07.035>
- [10] N. Kharoua, L. Khezzar, Z. Nemouchi, *Pet. Sci. Technol.* **2010**, *28* (7), 738–755. DOI: <https://doi.org/10.1080/10916460902804721>
- [11] R. Sabbagh, M. G. Lipsett, C. R. Koch, D. Nobes, in *Proc. of the Int. Mechanical Engineering Congress and Exposition*, Montreal **2014**.
- [12] D. Stanbridge, R. Swanborn, C. P. Heijckers, Z. Olujić, *Comput. Aided Chem. Eng.* **2000**, *8*, 391–396. DOI: [https://doi.org/10.1016/S1570-7946\(00\)80067-X](https://doi.org/10.1016/S1570-7946(00)80067-X)
- [13] A. Belaidi, M. Thew, *Chem. Eng. Res. Des.* **2003**, *81* (3), 305–314. DOI: <https://doi.org/10.1205/02638760360596856>
- [14] M. Bennett, R. Williams, *Miner. Eng.* **2004**, *17* (5), 605–614. DOI: <https://doi.org/10.1016/j.mineng.2004.01.021>
- [15] M. Meyer, M. Bohnet, *Chem. Eng. Technol.* **2003**, *26* (6), 660–665. DOI: <https://doi.org/10.1002/ceat.200390100>
- [16] E. Perfect, C. Rowley-Williams, C. Mackenzie, A. Moussavi, *US Patent 9 005 988-B2*, **2015**.
- [17] P. Lambert, *J. Hazard. Mater.* **2003**, *102* (1), 39–55. DOI: [https://doi.org/10.1016/S0304-3894\(03\)00201-2](https://doi.org/10.1016/S0304-3894(03)00201-2)
- [18] P. Durdevic, C. Raju, M. Bram, D. Hansen, Z. Yang, *Sensors* **2017**, *17* (1), 124. DOI: <https://doi.org/10.3390/s17010124>
- [19] S. D. Fowler, P. Greenspan, *J. Histochem. Cytochem.* **1985**, *33* (8), 833–836. DOI: <https://doi.org/10.1177/33.8.4020099>
- [20] T. Hagemeyer, R. Bordás, K. Zähringer, D. Thévenin, *Exp. Fluids* **2014**, *55* (1), 1639. DOI: <https://doi.org/10.1007/s00348-013-1639-7>
- [21] T. Hagemeyer, M. Hartmann, M. Kühle, D. Thévenin, K. Zähringer, *Exp. Fluids* **2012**, *52* (2), 361–374. DOI: <https://doi.org/10.1007/s00348-011-1232-x>
- [22] R. T. Kollholl, K. Kelemen, H. P. Schuchmann, *Chem. Eng. Technol.* **2015**, *38* (10), 1774–1782. DOI: <https://doi.org/10.1002/ceat.201500318>
- [23] M. Kraume, *Mischen und Rühren*, Wiley-VCH Verlag, Weinheim **2003**.